Iron oxide/PLGA nanoparticles for magnetically controlled drug release

+

IRON OXIDE/PLGA NANOPARTICLES FOR MAGNETICALLY CONTROLLED DRUG RELEASE

M. Rosaria Ruggiero[1,2], Simonetta Geninatti Crich[1], Elisabetta Sieni[3], Paolo Sgarbossa[3], E. Cavallari[1], Rachele Stefania [1], Fabrizio Dughiero[3], Silvio Aime[1].
[1]University of Turin, Department of Molecular Biotechnology and Health Sciences - Turin, Italy; [3] SAET S.p.A- Leinì (To) Italy; [2] University of Padua, Department of industrial engineered – Padua.

ABSTRACT

Recently, nanoscale stimuli-responsive devices have received much attention thanks to their potential to limit the cytotoxic effect of the therapeutic treatment at the diseased tissue. Among different physical triggers, large alternating magnetic fields enable the conversion of magnetic energy into heat by using magnetic nanoparticles that generate localized hyperthermia, named Magneto Fluid Hyperthermia (MFH). This methodology can be exploited for cancer therapy or/and thermally activated drug release. The small size iron oxide nanoparticles (Fe-NPs), such as SPIO (small iron oxide particles) and USPIO (ultra-small iron oxide particles), currently used for this application have many limitations due to their 1)high intratumor concentration needed due to the low heating power 2)short particle blood-half-life, 3)non-specific distribution, 4)low internalization efficiency. For these reasons many efforts are necessary to make magneto fluid particle hyperthermia (MFH) a competitive tumor therapy for clinical applications. New iron oxide nanoparticles, coated with oleate, with a diameter of 5-18 nm, have been prepared by co-precipitation and incorporated into PLGA-NPs (PLGA=Poly(lactic-co-glycolic acid) in order to improve their biocompatibility and “in vivo” stability. Moreover, PLGA-NPs have been loaded with both NPs-Fe and antitumor drugs (Paclitaxel, PTX), an anticancer hydrophobic drug used in the treatment of ovarian and breast cancer, to perform MFH triggered drug release. The PTX and Fe-NPs loaded nanoparticles may be considered as an effective anticancer drug delivery system for Imaging-guided hyperthermic treatment of tumors.

INTRODUCTION

Biological applications of nanotechnology have become the central focus in cancer treatment and research due to their potential in detecting cancer at the cellular scale (early stage), entering the region, and destroying the cells before they start to proliferate to form a tumor mass [1].

The use of hyperthermia treatment as an adjuvant for cancer therapies has been known since 3000 BC when some patients were treated by using hot sand baths and saunas [2]. Between the range of 40°C and 43°C, the majority of cancer cells tend to die by activation of several biochemical processes, firstly with enhanced production of heat shock protein (hsp), while healthy cell survive [3].

Hyperthermia may be induced locally, regionally or in the whole body for the treatment of tumor [4]. Local hyperthermia induces the least severe side effects and it is performed by wide different approach, including radiofrequency ablation, focused ultrasound, laser ablation and, recently, Magnetic Fluid Hyperthermia [5].

Magnetic fluid hyperthermia (MFH) is one of clinical nanotherapies, recently approved in Europe for treatment of glioblastoma and used in some clinical trials by MagForce (Berlin, Germany) to treat prostate and pancreatic cancer [6]. It relies on the use of magnetic nanoparticles (MNPs) as heat generators to induce localised cell death by the application of external alternating magnetic field (AMF) [7]. Different mechanisms are responsible for the thermal energy generated by magnetic nanoparticles after application of an AMF. They are strongly related to the magnetic properties of magnetic nanoparticles (i.e. the overall magnetization (M_s), and the effective anisotropy constant (K_{eff})) that are strictly dependent on their size, shape and composition [8]. In particular, the mechanism of energy dissipation can either be through Néel relaxation, the rapid internal re-orientation of particle's magnetic moment with the applied field, or Brownian relaxation, frictional heating caused by physical rotation of magnetic particles [9]. The effective relaxation time (τ) of the magnetic particles is defined, in following equation (1), as

$$\frac{1}{\tau} = \frac{1}{\tau_N} + \frac{1}{\tau_B} \quad (1)$$

where τ_N and τ_B are the Néel and Brownian magnetic relaxation times, respectively. The shorter relaxation time determines the dominant relaxation mechanism. τ_N and τ_B magnetic relaxation times of a particle are given by the following equations (2) and (3)[9]:

$$\tau_N = \tau_0 \, exp \frac{KV_M}{kT} \quad (2)$$

$$\tau_B = \frac{3\eta V_H}{kT} \quad (3)$$

where $\tau_0 = 10^{-9}$ s, K the anisotropy constant, V_M the volume of particle, k the Boltzmann constant, T the temperature, η the viscosity and V_H the hydrodynamic particle volume.

The relative contribution arising from Néel and Brown relaxation processes depend on the particle size, shape and chemical characteristics. The Néel time has an exponential dependence on magnetic anisotropy and particle volume, whereas the Brownian correlation time varies linearly with particle volume and solvent viscosity [10]. Furthermore, theoretical and experimental results strongly suggest that highly efficient intracellular hyperthermia modality can be achieved by exploiting the Néel rather than the Brown relaxation.

MNPs are single or multiple inorganic crystal of a magnetic material that offer some attractive possibilities in biomedical applications, such as magnetic separation, drug delivery, hyperthermia treatments and Magnetic Resonance Imaging (MRI) contrast enhancement [4]. For most biomedical application the MNPs are made from ferromagnetic iron oxide, such as magnetite (Fe_3O_4) and magnemite (γ-Fe_2O_3) as they precisely respond to external magnetic fields by mechanical motion or dissipation of thermal energy through relaxation losses [11]. The small sized iron oxide nanoparticles (Fe-NPs), such as SPIO and USPIO, clinically approved for MRI and hyperthermia application have many limitations due to their high intratumor concentration needed as a consequence of the low heating power and their non-specific distribution [12]. For these reasons many efforts are necessary to make magneto fluid particle hyperthermia (MFH) a competitive tumor therapy for clinical applications. Moreover, it is crucial for the development of MFH to rely on analytical methods able to characterize new magnetic nanoparticles and to predict their heating capacity in physiological conditions.
In this study, the MFH properties of newly prepared iron oxide nanoparticles (MNPs), coated with oleate moieties and prepared by co-precipitation method have been evaluated. Since these particles are completely insoluble in water, they were incorporated into PLGA (Poly (lactic-co-glycolic acid) nanoparticles (PLGA-MNPs). The incorporation of magnetic nanoparticles inside PLGA-NPs has many advantages [13] 1) it improves the magnetic nanoparticles stability and bioavailability; 2) it allows their efficient dispersion in water; 3) it avoids their aggregation; 4) it hampers the Brownian relaxation by blocking magnetic nanoparticles inside the PLGA-MNPs solid core thus allowing Néel relaxation, also in the presence of larger particles. The results from the "in vitro" characterization can be immediately used for foreseeing the "in vivo" behaviour. The correlation between the field dependence of the longitudinal relaxation rate (R_{1obs}), described by the so-called Nuclear Magnetic Resonance Dispersion (NMRD) profile, for nanoparticles and their heating power has been investigated. For iron oxide particles the inner sphere contribution to the water protons relaxation is negligible whereas the outer sphere term is the dominant one [14], essentially due to the diffusion of the water protons near the local variable magnetic field generated by the paramagnetic ion. Thus by analysing the dipolar interaction between proton spins and the magnetic moment it is possible to extrapolate important information about the magnetic nanoparticles, namely, their average radius r, their specific magnetization M_s, their anisotropy energy E_a, and their Néel relaxation time τ_N that determine the heating potential of the magnetic nanoparticles. Thus, supermagnetic nanoparticles are mostly used like negative contrast agent both in molecular and cellular imaging because of their negative enhancement effect on T_2- and T_{2*}-weighted images [15]. Taking advantage of this feature, to combine imaging and therapeutic allows and to create a theranostic agent, PLGA-MNPs have been loaded also with an anticancer hydrophobic drug currently used in the treatment of ovarian and breast cancer (Paclitaxel, PTX)(figure 1), in which, however, the drug release is triggered MFH [16].

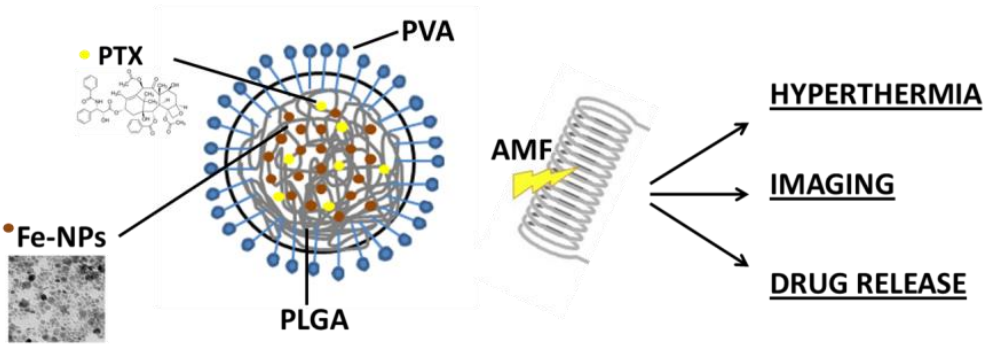

Figure 1: A schematic representation of PLGA-MNPS-PTX and fields of application of this system

RESULTS AND DISCUSSION

Synthesis of MNPs and PLGA-MNPs

The iron oxide magnetic nanoparticles (MNPs) used for the preparation of the PLGA nanocomposites (PLGA-MNPs) have been obtained by the co-precipitation in basic conditions from an iron (II/III) chlorides containing solution [17]. The size and morphology of the magnetic nanoparticles have been characterized by means of a TEM analysis (Figure 2 A). For each sample the average size has been evaluated using ImageJ software and the average particle sizes are 9.7±2.8 (83%) and 18±1.7 (17%). As expected by nanoparticles obtained by co-precipitation a high dispersity and a large average diameter were observed [14].

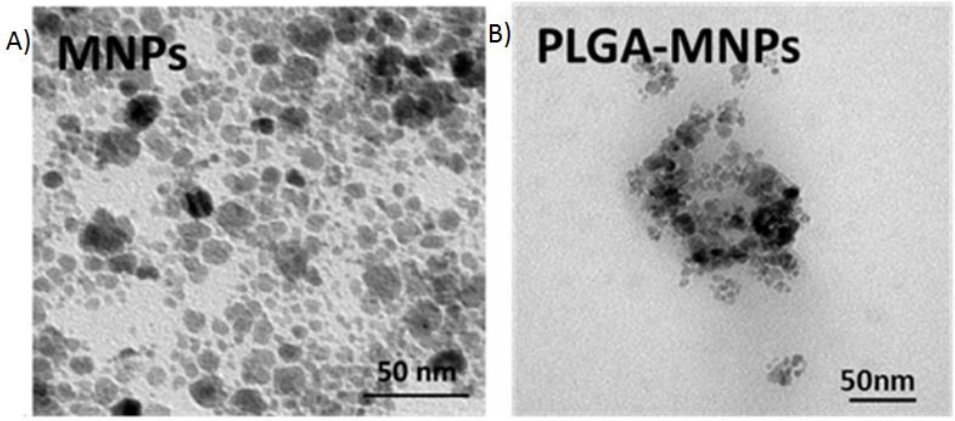

Figure 2: The TEM analysis of MNPs and PLGA-MNPs

PLGA-MNPs were obtained by the o/w emulsion solvent extraction method [18]. The organic phase was prepared by dissolving PLGA RG 502H, MNPs and paclitaxel (PTX) in chloroform. The water phase was a poly (vinyl alcohol) (PVA) aqueous solution. PVA is the most commonly used emulsifier for the preparation of PLGA-MNPs because it yields particles that are relatively uniform, small sized, and easy to be re-dispersed in water [18]. The organic phase was added to the aqueous phase, and the resulting mixture was extensively sonicated. The nanospheres were obtained by slow organic solvent evaporation of the o/w emulsion. The iron encapsulation yield in PLGA-Fe-NPs is 68±9 %, determined by ICP-MS, while for PTX is 40±12%, determined by HPLC [14]. The average hydrodynamic diameters of PLGA-Fe-NPs have been obtained by dynamic light scattering (DLS) measurements, and they are 164±12 nm. In figure 2 the TEM image of PLGA-MNPs is reported. Figure 3 displays the T_1 magnetic field dependence (NMRD) of PLGA-MNPs [14].

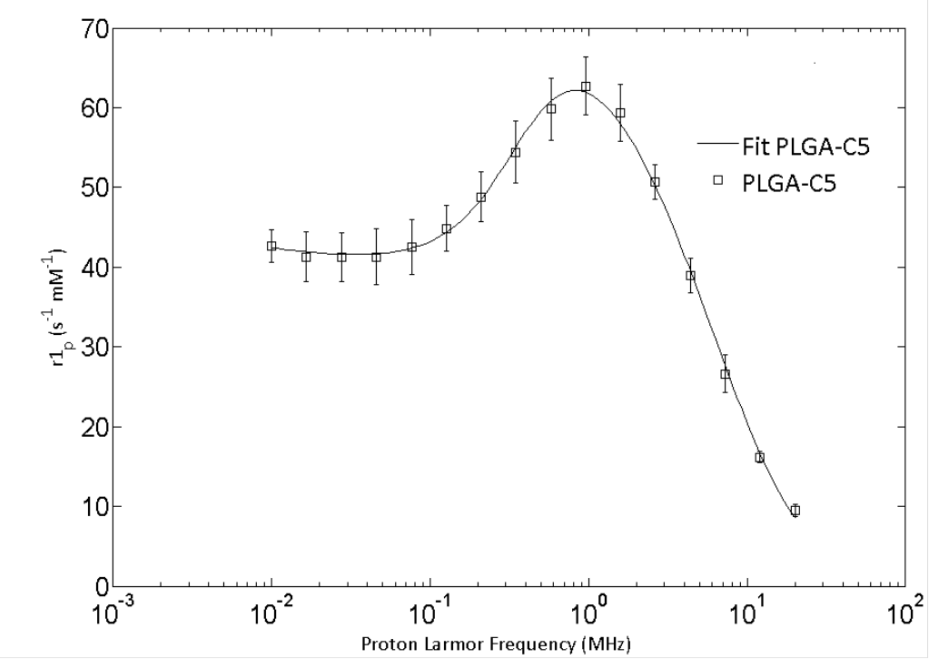

Figure 3: NMRD profiles of PLGA-MNPs

The shape of the curves is typical of the relaxation induced by superparamagnetic particles, i.e. the loading into the PLGA matrix seems to not affect the overall magnetic properties of the iron oxide particles. The water proton longitudinal relaxation arises from the dipolar interaction between the magnetic moments of water protons and the electron magnetic moment of the iron oxide particles and it is modulated by Néel relaxation (flip of the particle magnetic moment from different anisotropy directions) and water diffusion. At low magnetic fields, for particles with a diameter > 15 nm, the high crystal anisotropy maintains the particle magnetic moment locked onto the anisotropy axis. Since they can flip from one easy direction to another, the relaxation can occur through either Néel relaxation or water diffusion. On the contrary, at high magnetic fields, the Néel relaxation is not possible since the magnetic moment is locked onto the magnetic field direction and the modulation is due to water diffusion (τ_D). For very small particles, characterized by smaller anisotropy energy, the locking of the particle magnetization onto the anisotropy directions does not occur and Néel relaxation becomes negligible also at low magnetic fields [14].
The NMRD profiles are fitted using the Roch's heuristic model [19], modified by Lascialfari et al[20] that has been developed for particle core diameter < 20nm. Fitting equations have been written using Matlab and obtained data are reported in table [14].

	r_{TEM} [nm]	r_{NMRD} [nm]	τ_D [ns]	$M_{S,NMRD}$ [emu g^{-1}]	τ_N [s rad^{-1}]
PLGA-C5	9.0 ± 0.9	13.2 ± 0.3	75.8 ± 3.9	62.1 ± 2.6	2.73 ± 0.48 x 10^{-7}

Table 1: The data obtained by fitting equations

Assessment of magnetic hyperthermia properties

To assess hyperthermia capability of the PLGA-MNPs, they were exposed to a time varying magnetic field. The device to apply the time-varying magnetic field to magnetic nanoparticles is composed by a voltage generator EASYHEAT 8310 LI connected to a cylindrical inductor. The EASYHEAT 8310 LI supplies the inductor with a voltage up to 700 V_{rms} in a frequency

range between 150 and 400 kHz, inductor designed to have a uniform magnetic field by means of finite element codes and optimization codes [21]. The copper inductor is a cylindrical solenoid with 7 turns, an internal diameter of 8 cm and a length of 15 cm. The sample is logged in Teflon container where a 5 ml glass vial is screwed to the cup of the container. The temperature is measured by means of an Optocom Fotemp-1H thermometer with a TS3/2 fiber optic. The fiber optic is inserted in the 5 ml glass vial by means of a hole in the center of the cup. The temperature is sampled with a time step of 1^{-s}. The solutions were placed in an AC magnetic field of frequency (ν = 177 kHz, amplitude H_0 = 18 kA/m; corresponding to a product $H_0\ \nu = 2.4x10^9$ A m^{-1} s^{-1}).The temperature increase generated by heat dissipation was recorded as a function of time of exposure to the AMF for 5min and 30min (figure 4 A and B).

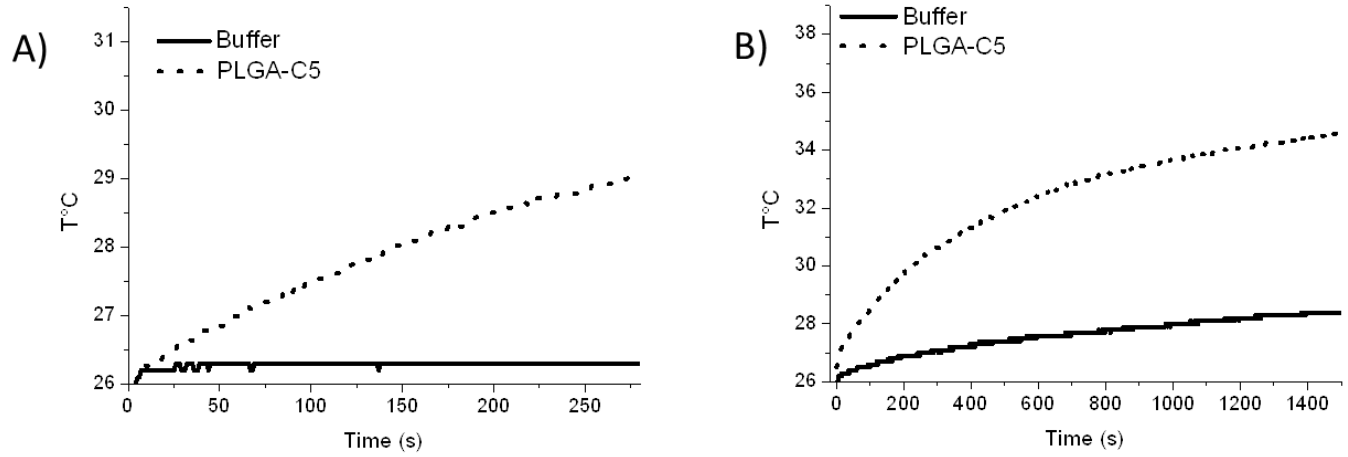

Figura 4: Temperature increase as a function of time after exposition for 5min (A) and 30min (B) to AMF

Typically, hyperthermal efficiency of a material is reported in terms of the specific absorption rate (SAR), reported in equation (4)

$$SAR = C\ \frac{m_{sample}\,\Delta T}{m_{iron}\Delta t} \quad (4)$$

where C is the heat capacity of the suspension, m sample is the mass of the sample, m_{iron} is the mass of iron, and Δt is the initial slope of the time-dependent heating curve, respectively [7]. The $\Delta T/\Delta t$ value was calculated by taking the initial slope of the temperature increase (50-150s) as in this time range the temperature increase was linear. The SAR value calculated for PLGA-MNPs is 34.57±2.25 W/g.

"In vitro" Paclitaxel release triggered by MFH

Figure 5 shows the amount of PTX released by PLGA-MNPs after 30min or 5min of AMF exposure. The *"In vitro"* release of drug from treated nanoparticles was estimated in Phosphate Buffer Saline (PBS) at 6, 24 and 48h after AMF exposure. The heat produced during the MFH treatment is sufficient to destabilize PLGA-MNPs triggering their selective drug release that is significantly higher after 30 min of exposition to AMF than that measured on both control and on samples exposed to same magnetic field only for 5min [14].

PLGA-MNPs loaded with PTX at concentration of 2,3 μg/ml of drug were diluted in PBS (2ml) and transferred to dialysis bags placed in PBS (50ml) with magnetic stirring at 110

rpm/37 °C. At appropriate intervals, the buffer solution was replaced with fresh PBS, and the concentration of the released PTX in the removed PBS was determined by HPLC [14].

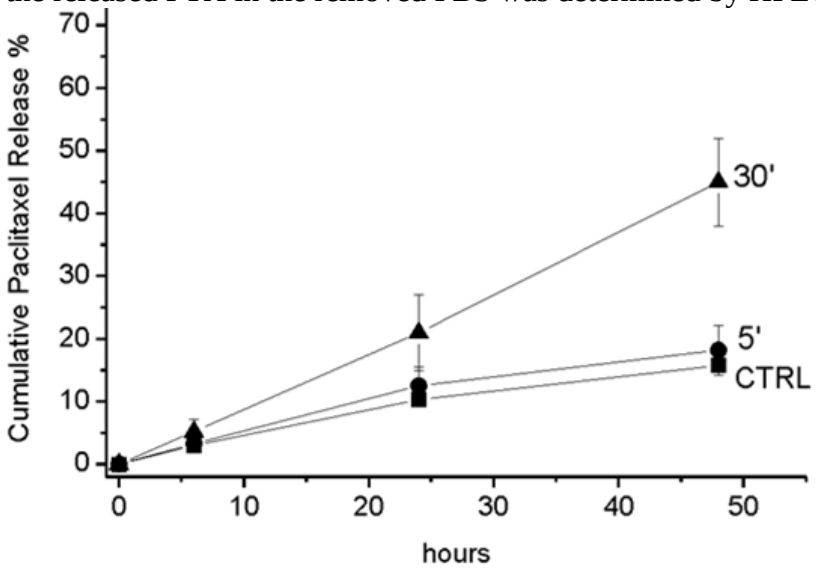

Figure 5: Release of PTX after AMF exposition at different time intervals

Magnetic Resonance Imaging of PLGA-MNPs on cell lines

PLGA-MNPs are evaluated as negative contrast agent for MRI and, eventually, as report in real time of *in vivo* distribution of both MNPs and the drug with which they are loaded.

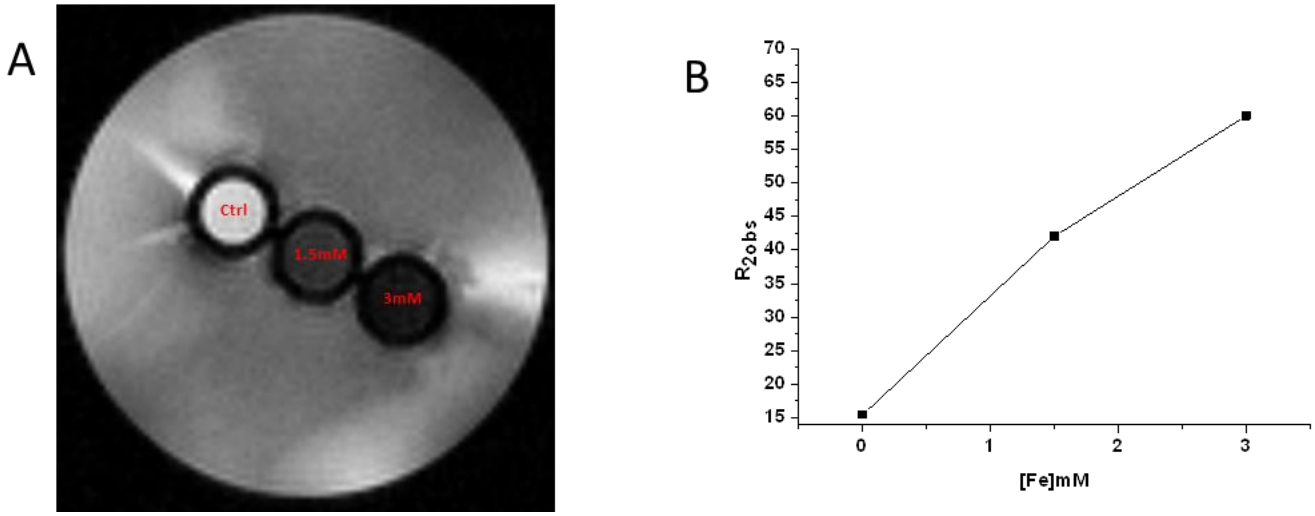

Figure 6: T_2-weight image (A) and R_{2obs} (B) of A549 cell line as function of concentration of iron

A549, human alveolar basal epithelial adenocarcinoma cells, are incubated with PLGA-MNPs at different concentrations of iron for 24h. A T_2-weighted MR image of an agar phantom containing A549 cells are acquired at 7T (Fig.6A). The graph of figure 6B shows the relaxation rates (R_{2obs}) determined by MRI as a function of incubated iron concentration. By ICP-MS the iron concentration inside the cell due to aspecific endocytosis of PLGA-MNPs after 24h incubation was determined. The internalized iron was 6.4±2.4*10-9mol/mg of proteins that correspond to a concentration of 140±51 µM of iron inside the cellular pellet. Unfortunately, this concentration seems to be too low to obtain a detectable heating effect. However, Gordon et al. [22] suggested that internalised MNPs could be more effective at

killing cancer cells because the cell membrane would act as an insulator enhancing the hyperthermic effect [4].
With the advent of nanotechnology and the possibility of targeting MNPs to specific structures within the cell, the idea of selective destruction of these intracellular targets has become more attractive realized local heating and killing cancer cells without the need for a macroscopic temperature increase [4].

CONCLUSIONS

Preliminary studies, herein reported, have shown that new nanosystems loaded with Fe-NPs and Paclitaxel appear very promising for designing innovative "theranostic" applications. Furthermore the encapsulation of iron oxide inside the PLGA allows the characterization of insoluble MNPs and predicts hyperthermia efficiency, not hampered triggered release of drug from PLGA-NPs by MFH. Furthermore, with MRI the measurement of their concentration before the AFM treatment is possible. This permits to find the best time to perform the treatment thus increasing the probability of its success.

REFERENCES

[1] N. Saniei, Hyperthermia and Cancer treatment, Heat transfer Engineering, 30 (2009), 915-917.
[2] G.F. Goya, Cell death induced by AC magnetic fields and magnetic nanoparticles: current state and perspectives, International Journal of Hyperthermia, 29 (2013), 810-818.
[3] G. Baronzio, A brief overview of hyperthermia in cancer treatment. Journal Integral Oncology, 3(2014), 115.
[4] B. Kozissnik, Magnetic fluid hyperthermia: advances, challenges, and opportunity, International Journal of Hyperthermia, 29 (2013), 706-714.
[5] A. Chicel, Hyperthermia- Description of a method and review of clinical applications, Reports of Practical Oncology & Radiotherapy, 12 (2007), 267-75.
[6] U. Gneveckow, Description and characterization of the novel hyperthermia thermoablation system MFH 300F for clinical magnetic fluid hyperthermia. Medical Physics, 31(2004), 1444-1451
[7] S. Kossatz, High Therapeutic efficiency of magnetic hyperthermia in xenograft models achieved with moderate temperature dosages in the tumor area. Pharmaceutical Research 31 (2014), 3274-88.
[8] R. Hergt, Magnetic particle hyperthermia: nanoparticle magnetism and materials development for cancer therapy, Journal of Physics: Condensed Matter, 18 (2006), S2919–S2934
[9] M. Suto, Journal of Magnetism and Magnetic Materials, 321 (2007), 1493–1496.
[10] S. Laurent, Chemical Reviewers, 108 (2008), 2064-110.
[11] Q.A. Pankhurst, Progress in applications of magnetic nanoparticles in biomedicine, Journal of Physics D: Applied Physics, 42 (2009), 224001.
[12] S. Laurent, Superparamagnetic iron oxide nanoparticles: promises for diagnosis and treatment of cancer, International Journal of Molecular Epidemiology and Genetics. 2 (2011), 367–390.
[13] F. Danhier, PLGA-based nanoparticles: An overview of biomedical applications, International of Journal of controlled release, 161 (2012), 505-522.
[14] M.R. Ruggiero, Magnetic hyperthermia efficiency and ^{1}H-NMR relaxation properties of iron oxide/paclitaxel-loaded PLGA nanoparticles, Nanotechnology 27 (2016), 285104.
[15] C. Corot Recent advances in iron oxide nanocrystal technology for medical imaging. Advanced Drug Delivery Reviews. 58 (2006), 1471-1504.

[16] SH Hu, Core-shell nanocapsules stabilized by single-component polymer and nanoparticles for magneto-chemotherapy/hyperthermia with multiple drugs, Advanced Materials, 24 (2012), 3627-32.
[17] E. Ghasemi, Synthesis and rheological properties of an iron oxide ferrofluid, Journal of Magnetism and Magnetic Materials, 320, (2008), 2635-2639.
[18]R.N. Mariano, Design of PLGA Based Nanoparticles for Imaging Guided Applications, Molecular Pharmaceutics 11 (2014), 4100-4106.
[19] A. Roch, Proton magnetic relaxation in superparamagnetic aqueous colloids: a new tool for the investigation of ferrite crystal anisotropy, Journal of Magnetism and Magnetic Materials, 201 (1999), 77-79.
[20] L. Bordonali, NMR-D study of the local spin dynamics and magnetic anisotropy in different nearly monodispersed ferrite nanoparticles, Journal of Physics: Condensed Matter, 25 (2013),066008.
[21] P. Di Barba, Optimal design of inductors for magnetic- fluid hyperthermia by means of migration- assisted NSGA, International Journal of Applied Electromagnetics and Mechanics., 51 (2016), 125–S134,
[22] RT. Gordon, Intracellular hyperthermia a biophysical approach to cancer treatment via intracellular temperature and biophysical alteration, Medical Hypotheses, 5 (1979),83-102.